

~~CONFIDENTIAL~~

6008
MAR 1958
Copy 2
RM L57



0144706

NACA RM L57L09

7825

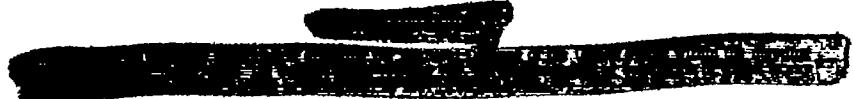


RESEARCH MEMORANDUM

MEASUREMENTS OF AERODYNAMIC HEAT TRANSFER IN
TURBULENT SEPARATED REGIONS AT A
MACH NUMBER OF 1.8

By Benjamine J. Garland and James R. Hall

Langley Aeronautical Laboratory
Langley Field, Va.

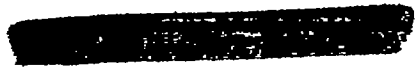


NATIONAL ADVISORY COMMITTEE FOR AERONAUTICS

WASHINGTON

February 20, 1958

~~CONFIDENTIAL~~



Classification of record (such as to Unclassified)

By authority of Nasa Tech Pub Announcement #45
(OFFICER AUTHORIZED TO CHANGE)

By AK
NAME AND

.....
GRADE OF OFFICER MAKING CHANGE)

..... 17 May 61
DATE



NATIONAL ADVISORY COMMITTEE FOR AERONAUTICS

RESEARCH MEMORANDUM

MEASUREMENTS OF AERODYNAMIC HEAT TRANSFER IN
TURBULENT SEPARATED REGIONS AT A
MACH NUMBER OF 1.8

By Benjamin J. Garland and James R. Hall

SUMMARY

An exploratory investigation of the aerodynamic heating in the regions of separated and reattached flow on a 4° half-angle cone behind oversized nose tips of various shapes and sizes was conducted in a free jet at a Mach number of 1.8. The Stanton numbers in the separated flow behind the nose tip were reduced to about one-half of the theoretical turbulent boundary-layer values in some cases. The Stanton numbers behind the reattachment point agreed with the turbulent theory. Reattachment did not cause a local hot spot.

INTRODUCTION

Recently, considerable attention has been given to the heat transfer for a separated flow. It has been shown both analytically and experimentally (refs. 1 and 2) that, for laminar separation, large reductions in heat transfer are possible. Investigations at $M = 2.0$ and at high stagnation temperatures (achieved by chemical reaction) have indicated a relatively cool region on a cone behind an oversized spherical ceramic tip (ref. 3). These tests have prompted further investigations on separated flow, some of which are reported herein. Separated flow was achieved by mounting various oversized tips on an 8° total-angle cone instrumented with thermocouples. These tests were conducted in the preflight jet located at the Langley Pilotless Aircraft Research Station at Wallops Island, Va., for $M = 1.8$ and free-stream Reynolds numbers based on a length of 1 foot of 10×10^6 to 11×10^6 .

SYMBOLS

C_f	local skin-friction coefficient
c_p	specific heat of air, Btu/slug-°F
$c_{p,w}$	specific heat of wall material, Btu/lb-°F
d	diameter of tip, in.
l	characteristic length, in.
M	Mach number
N_{St}	Stanton number, $h/c_p \rho V$
R	Reynolds number, $\rho V l / \mu$
T	temperature, °R
t	time, sec
x	axial length along basic cone, in.
V	velocity, ft/sec
η_r	recovery factor
μ	viscosity of air, slugs/ft-sec
ρ	density of air, slugs/cu ft
ρ_w	specific weight of wall material, lb/cu ft
τ	skin thickness
Subscripts:	
aw	adiabatic wall
w	wall
t	stagnation
∞	free stream

MODELS, INSTRUMENTATION, AND TESTS

The models consisted of the sting plus the various tips shown in figure 1. The sting was a 4° half-angle cone made of 0.0315-inch-thick Inconel with four equally spaced rows of seven thermocouples 90° apart along its length. The thermocouples were of the iron-constantan type and were welded to the inside of the skin. The sting was previously used in the tests reported in reference 4.

There were nine different tips, which are shown in figure 1. All the tips were made of a low conductivity fiberglass-resin plastic, except the reference 4° half-angle cone tip which was made of steel. The plastic was used in order to reduce conduction effects between the tip and the cone steel. There was no instrumentation in any of the tips.

Tests were made in the 12- by 12-inch Mach number 1.8 nozzle of the preflight jet of the Langley Pilotless Aircraft Research Station at Wallops Island, Va. A photograph of a typical model in position just prior to a test is shown in figure 2. The models were fixed on the tunnel center line for all tests. Each test lasted for 70 seconds. Test conditions are listed in table I.

DATA REDUCTION AND ANALYSIS

Two typical temperature time histories are given in figure 3. Shown are the temperatures measured at one of the thermocouples at the first station for the test of the 4° half-angle (basic) cone and for the disk tip.

The recovery factors along the cone surface were computed for the different tips by using the equation

$$\eta_r = \frac{T_{aw} - T_\infty}{T_t - T_\infty}$$

The recovery temperature was computed at 60 seconds at which time the rate of change of temperature was close to zero. The recovery factors which were determined for the four thermocouples at each station showed no systematic variation around the cone and were within 1.5 percent of the average value at each station. Average values are presented in this report.

The Stanton numbers along the cone were based on free-stream conditions and were calculated by using the equation

$$N_{St} = \frac{c_p, w \rho_w T_w \frac{dT_w}{dt}}{(T_{aw} - T_w) (c_p \rho V)_{\infty}}$$

The Stanton numbers were calculated for five different times during the period of high heating for each thermocouple on several runs. There was no systematic variation around the cone, and the average of all the points differed very little from the average for any one thermocouple. On the basis of these results, the Stanton numbers at each station for the remaining runs were based on only one thermocouple. The times at which the Stanton numbers were calculated were chosen as soon as possible after the flow in the nozzle had been established so that the forcing function $(T_{aw} - T_w)$ was maximized and the conduction errors were minimized.

For purposes of comparison, theoretical values of the Stanton number for laminar and turbulent boundary layers on the basic cone and on the hemisphere-tipped cone were calculated by the methods of references 5 and 6 using cone theory. The free-stream Reynolds number used in these calculations was based on the length from the projected cone tip of $l = \frac{1}{12} (3.58 + x)$ for the basic cone and the contour length from the stagnation point around the hemisphere, and hence along the cone, or $l = \frac{1}{12} \left(\frac{\pi d}{4} + x \right)$ for the hemisphere-tipped cone. The theory for the hemisphere-tipped cone was expected to give only a level for the laminar and turbulent values. The relationship

$$N_{St} = 0.6C_f$$

was used as given by the modified Reynolds analogy of reference 7.

RESULTS AND DISCUSSION

Shadowgraphs of the flow in each of the tests are presented in figure 4. A shock caused by the lip of the nozzle can be seen impinging between stations 4 and 5. It appears to have no significant effect on the recovery factors or on the Stanton numbers subsequently discussed. The separated region appears to extend to the second thermocouple station behind the large sphere, the cylinder, the disk, and the 45° half-angle cone. The separated region definitely extends past the first thermocouple station for the other tips, with the exception of the small sphere, which is marginal.

CONFIDENTIAL

The recovery factors along the cone for the various tips are presented in figure 5. There appeared to be a tendency of the recovery factors to decrease a few percent between stations 1 and 3 and then level out or increase slightly. An exception to this tendency is noted for the large spherical tip. For the first station the large sphere, the disk, the small sphere, and the 30° half-angle cone produced the lowest recovery factors. Those shapes which produced the largest separated regions also had the lowest recovery factors along the entire length of the cone.

The Stanton numbers along the cone for the various tips are presented in figure 6. Also shown are the theoretical values for turbulent boundary layers for a basic cone and for a hemisphere-tipped cone and for a hemisphere-tipped cone with a laminar boundary layer. The results for the basic cone are in good agreement with the theory. After the first station the Stanton numbers behind all the oversized tips except the small sphere agreed with the theoretical heating values for the hemisphere-tipped cone with a turbulent boundary layer. This agreement is perhaps fortuitous since there is no reason to believe that the theory as calculated should give more than a rough estimate of the Stanton number.

The Stanton numbers measured at the first station, the percent of the value measured for the basic cone, and the percent of the value predicted by turbulent theory for hemisphere-tipped cone are given in the following table for each tip tested:

Tip	Measured Stanton number	Percent of value measured for basic cone	Percent of value predicted by turbulent theory for hemisphere-tipped cone
Basic cone	13.0×10^{-4}	---	--
Small sphere	13.5	104	68
Medium sphere	19.0	146	96
Large sphere	13.0	100	71
Hemisphere	14.2	109	72
Cylinder	18.1	139	91
Disk	10.6	82	53
45° half-angle cone	10.3	79	52
30° half-angle cone	16.3	125	81

It is predicted in reference 1 that the heating of a separated laminar flow will be 0.6 of the laminar boundary layer and that the heating of a separated turbulent flow will be 6.3 times that for a turbulent boundary layer at $M = 0$. It is noted that experiments indicate a marked decrease in heating to 2.8 times turbulent boundary-layer values at $M = 1.6$.

The variation of temperature along the cone was within the accuracy of the instrumentation and indicated no local hot spot due to flow reattachment.

CONCLUDING REMARKS

Exploratory tests have been made of the aerodynamic heating in the regions of separated and reattached flow on a 4° half-angle cone behind oversized nose tips of various shapes and sizes at $M = 1.8$. The Stanton numbers in the region of separated flow behind the nose tip were reduced to about one-half of the theoretical turbulent boundary-layer values in some cases. The Stanton numbers behind the point of reattachment agreed with the turbulent boundary-layer theory. Reattachment did not cause a local hot spot.

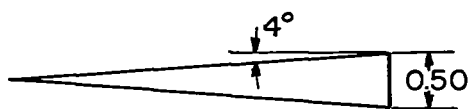
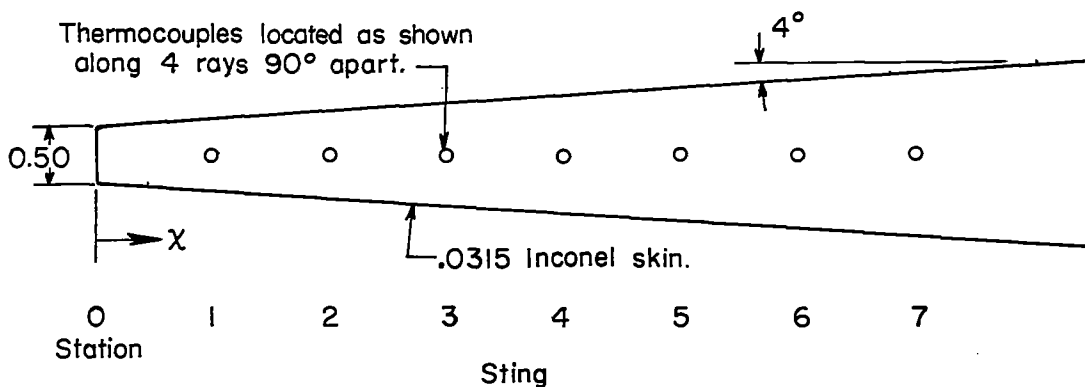
Langley Aeronautical Laboratory,
National Advisory Committee for Aeronautics,
Langley Field, Va., Nov. 14, 1957.

REFERENCES

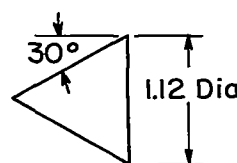
1. Chapman, Dean R.: A Theoretical Analysis of Heat Transfer in Regions of Separated Flow. NACA TN 3792, 1956.
2. Becker, John V., and Korycinski, Peter F.: Heat Transfer and Pressure Distribution at a Mach Number of 6.8 on Bodies With Conical Flares and Extensive Flow Separation. NACA RM L56F22, 1956.
3. Fields, E. M., Hopko, Russell N., Swain, Robert L., and Trout, Otto F., Jr.: Behavior of Some Materials and Shapes in Supersonic Free Jets at Temperatures up to 4,210° F, and Descriptions of the Jets. NACA RM L57K26, 1958.
4. O'Sullivan, William J., Chauvin, Leo T., and Rumsey, Charles B.: Exploratory Investigation of Transpiration Cooling To Alleviate Aerodynamic Heating on an 8° Cone in a Free Jet at a Mach Number of 2.05. NACA RM L53H06, 1953.
5. Van Driest, E. R.: Turbulent Boundary Layer in Compressible Fluids. Jour. Aero. Sci., vol. 18, no. 3, Mar. 1951, pp. 145-160, 216.
6. Van Driest, E. R.: Investigation of Laminar Boundary Layer in Compressible Fluids Using the Crocco Method. NACA TN 2597, 1952.
7. Rubesin, Morris W.: A Modified Reynolds Analogy for the Compressible Turbulent Boundary Layer on a Flat Plate. NACA TN 2917, 1953.

TABLE I.- TEST CONDITIONS

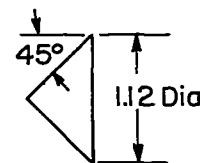
Tip	$T_t,$ °R	$T_\infty,$ °R	$\rho_\infty,$ slugs/cu ft	$V,$ ft/sec	R_∞ per foot
Basic cone	1,075	652	0.00219	2,250	11.2×10^6
Small sphere	1,054	642	.00204	2,230	10.5
Medium sphere	1,055	642	.00214	2,240	11.0
Large sphere	1,100	665	.00202	2,270	10.2
Hemisphere	1,085	658	.00206	2,270	10.4
Disk	1,065	645	.00206	2,245	10.5
Cylinder	1,100	673	.00200	2,290	10.2
45° half-angle cone	1,055	640	.00218	2,230	11.0
30° half-angle cone	1,130	684	.00218	2,310	11.0



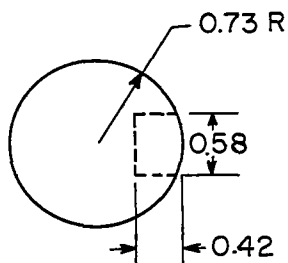
(a) Basic cone (steel).



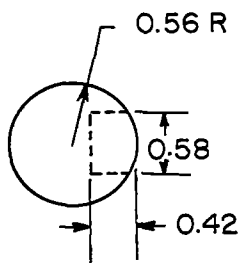
(b) 30° half-angle cone.



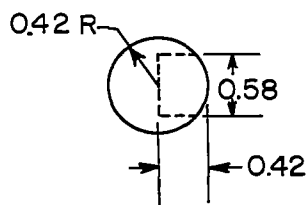
(c) 45° half-angle cone.



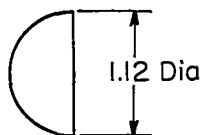
(d) Large sphere.



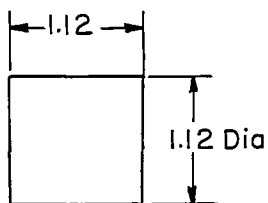
(e) Medium sphere.



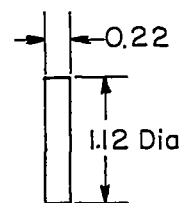
(f) Small sphere.



(g) Hemisphere.

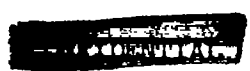


(h) Cylinder.



(i) Disk.

Figure 1.- Sting and tips employed in tests. All dimensions in inches. All tips made of fiberglass-resin plastic except basic cone.



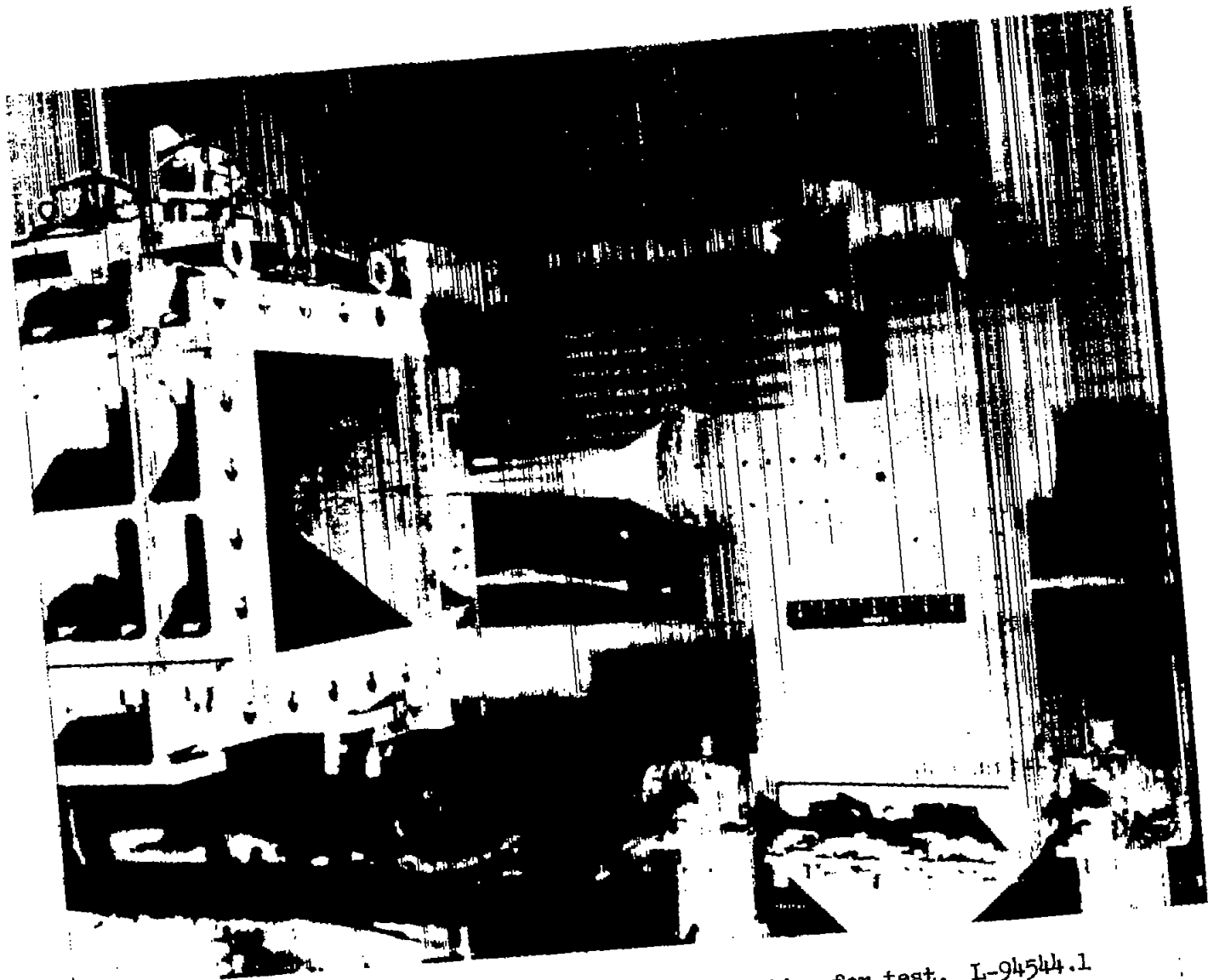


Figure 2.- Photograph of typical model in position for test. I-94544.1

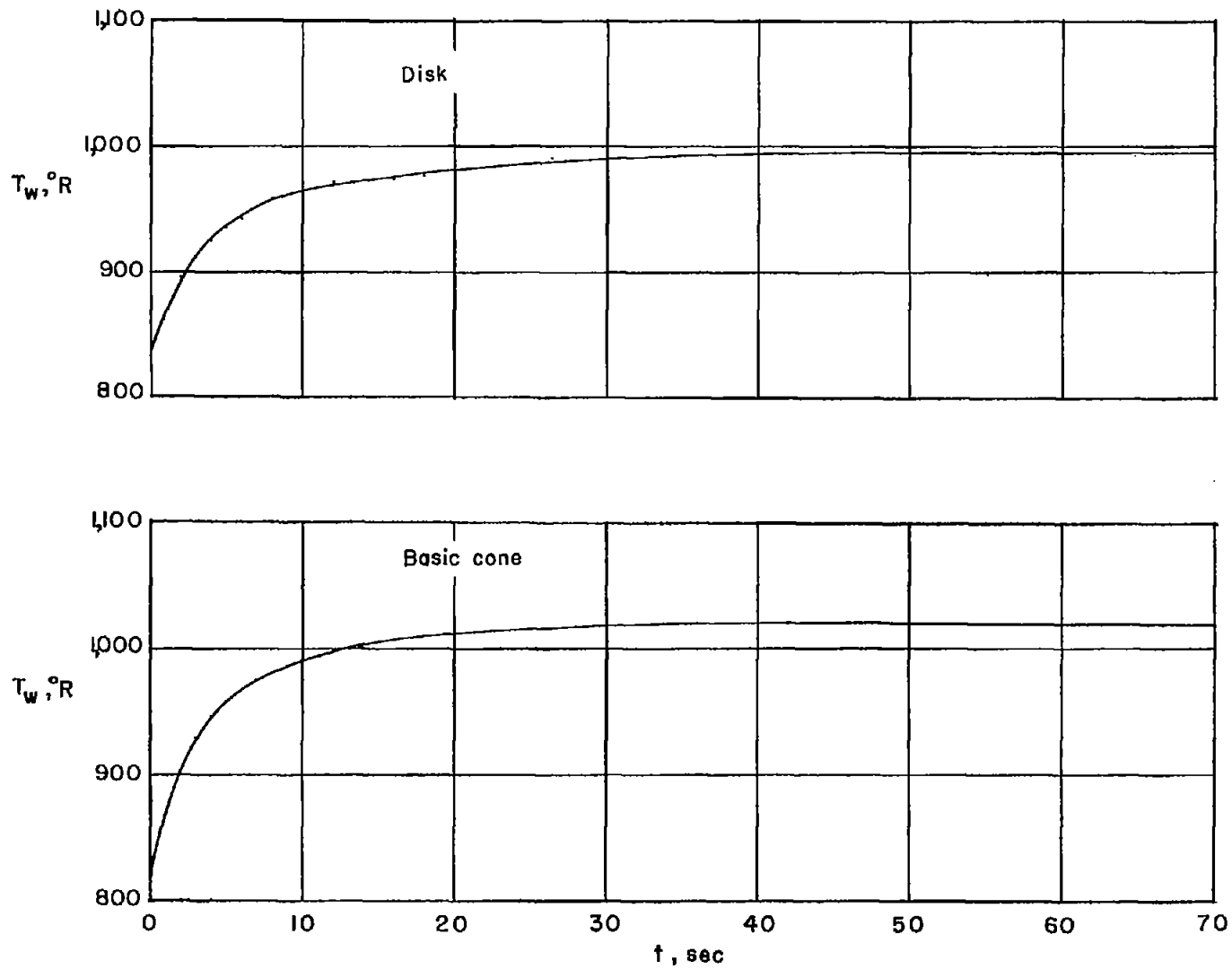
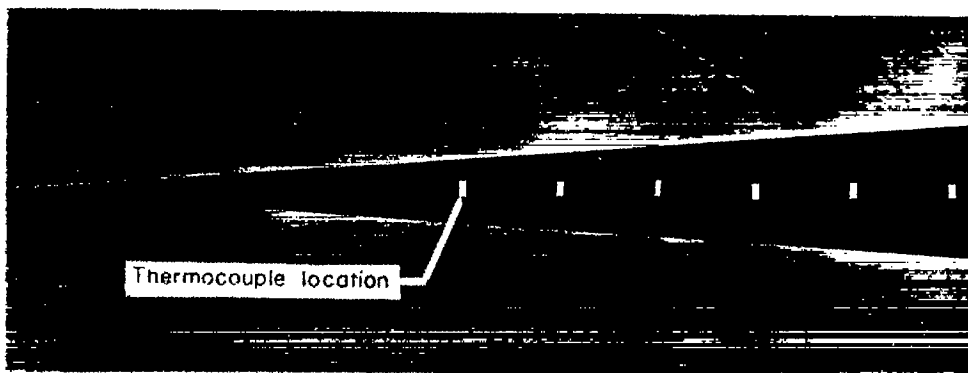
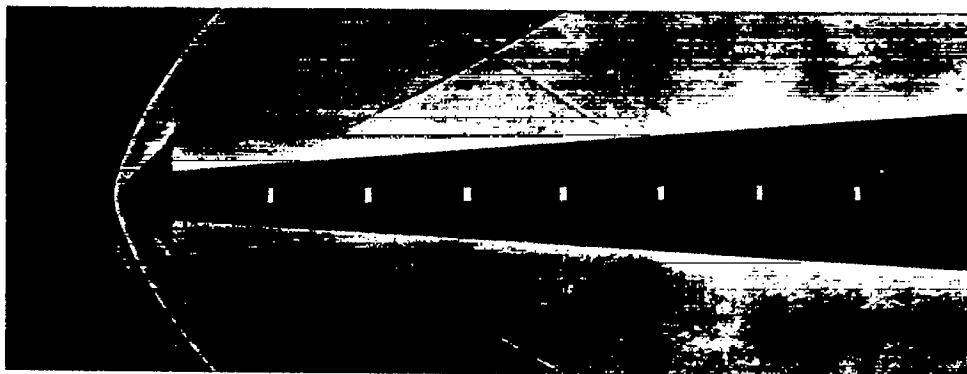


Figure 3.- Typical temperature time history of first station.



(a) Basic cone.

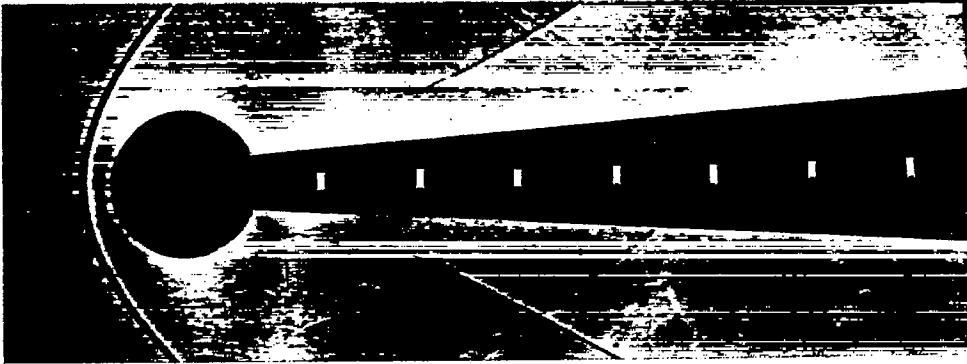


(b) 45° half-angle cone.

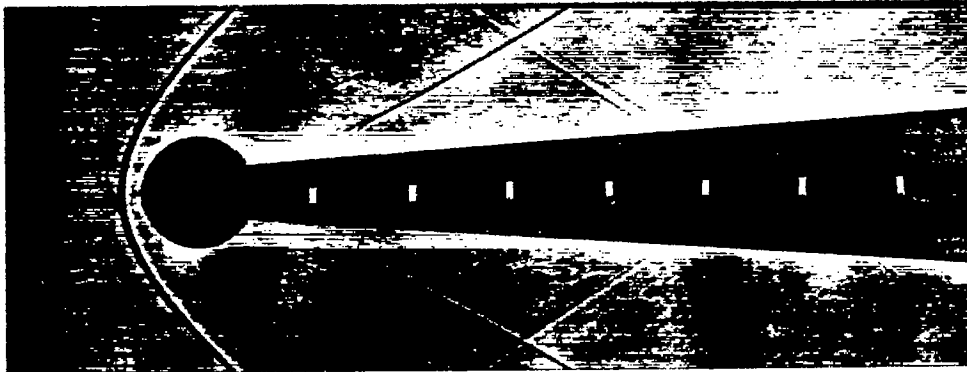


(c) 30° half-angle cone. L-57-4438

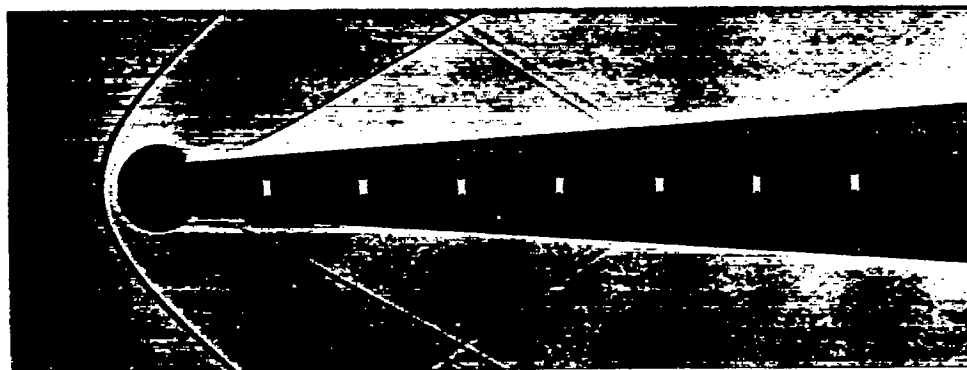
Figure 4.- Shadowgraphs of flow about the shapes tested.



(d) Large sphere.



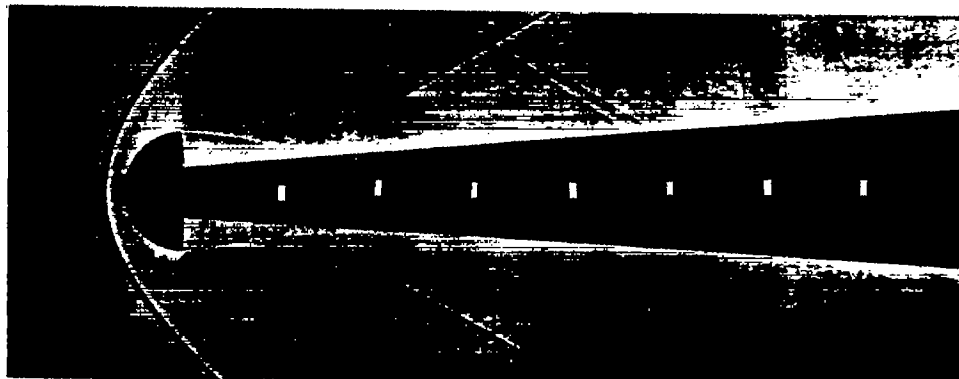
(e) Medium sphere.



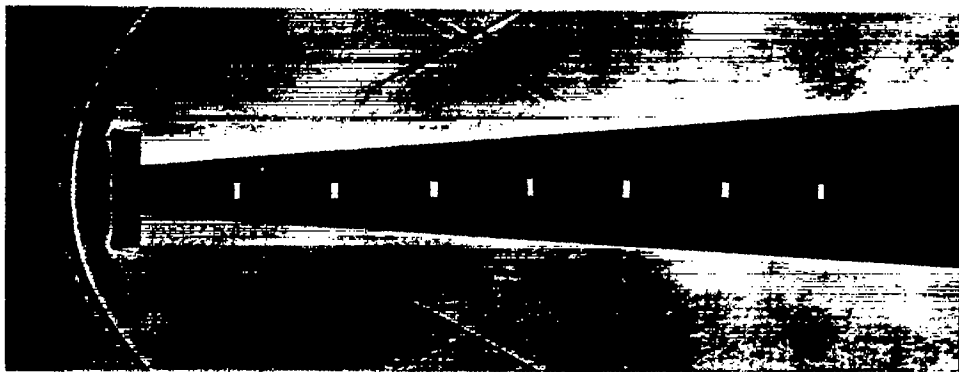
(f) Small sphere.

L-57-4439

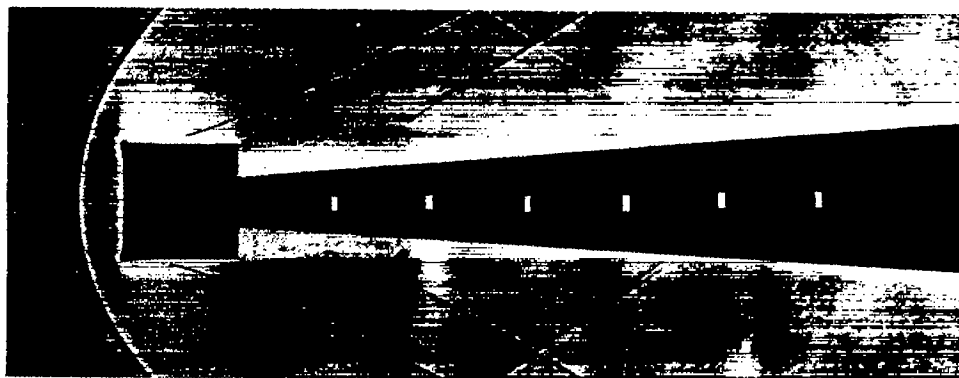
Figure 4.- Continued.



(g) Hemisphere.



(h) Disk.



(i) Cylinder.

L-57-4440

Figure 4.- Concluded.

- Basic cone
- Small
- ◇ Medium sphere
- △ Large sphere
- ▽ Hemisphere
- ▷ Cylinder
- ◻ Disk
- ◊ 45° Half-angle cone
- ◈ 30° Half-angle cone

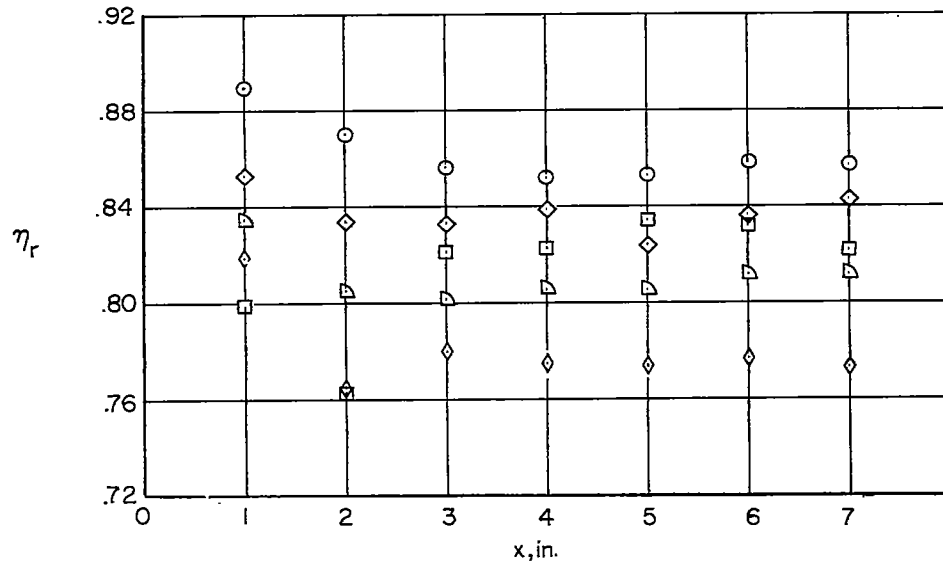
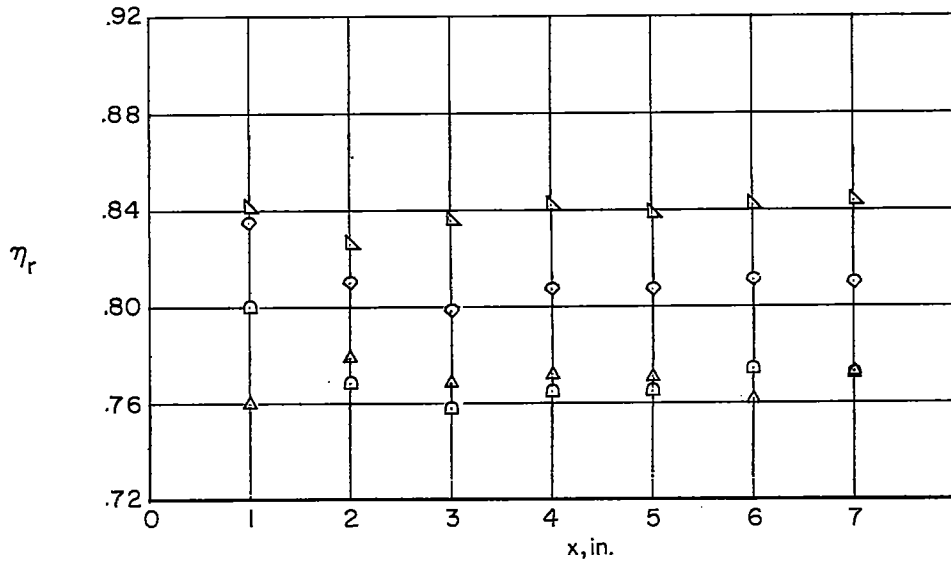


Figure 5.- Average recovery factor along cone for various tips shown in two charts for purposes of clarity.

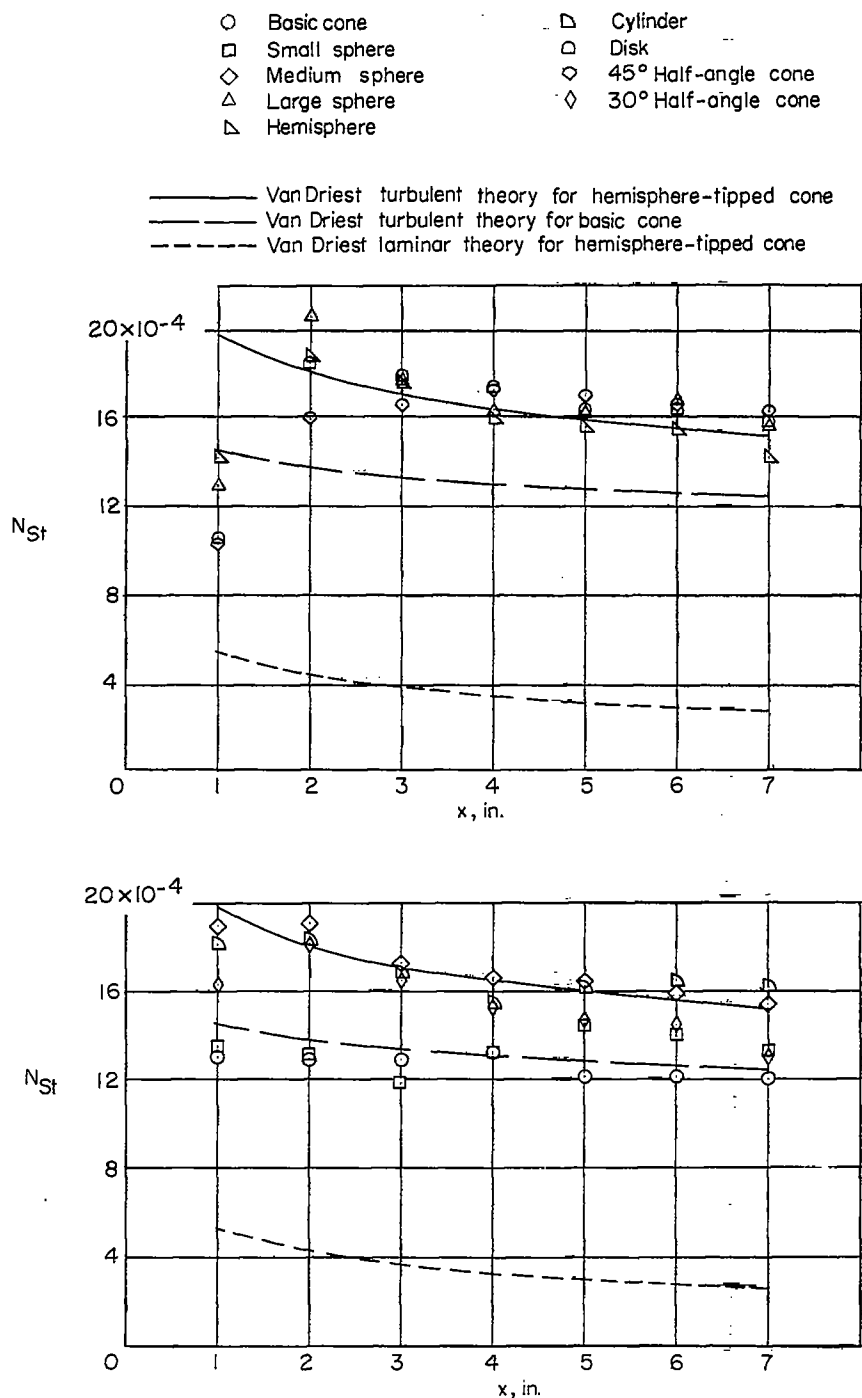


Figure 6.- Average Stanton number along cone for various tips shown in two charts for purposes of clarity.